ACTA ACUSTICA UNITED WITH ACUSTICA
Vol. 95 (2009) 744 – 752

DOI 10.3813/AAA.918202

Sympathetic String Modes in the Concert Harp

Jean-Loïc Le Carrou*, François Gautier
LAUM, CNRS, Université du Maine, Av. O. Messiaen, 72085 Le Mans, France. francois.gautier@univ-lemans.fr

Roland Badeau
TELECOM ParisTech (ENST) / CNRS LTCI, 46 rue Barrault, 75634 Paris Cedex 13, France

Invited paper based on a presentation at the International Congress on Acoustics in Madrid (ICA Madrid 2007)

Summary
The concert harp is composed of a soundboard, a cavity with sound holes and 47 strings. When one string is plucked, a number of normal modes involving the coupled motions of other strings are excited which induce a characteristic 'halo of sound'. This phenomenon, called sympathetic vibrations is due to a coupling between strings via the instrument's body. This coupling results in multiple spectral components in each partial of the resulting sound of the instrument. Resolution of Fourier analysis does not permit their identification. A high resolution Method (ESPRIT), was used to separate the spectral components which are very close one to another. Some of the measured spectral components in the analysed partials correspond to the response of sympathetic modes. The eigenfrequencies and mode shapes of these modes were investigated using a simplified model of the harp based on a waveguide approach in which bending and longitudinal motions of 35 strings connected to an equivalent beam representing the soundboard are described. Identified experimental sympathetic modes are very well captured by the model.

PACS no. 43.75.Gh

1. Introduction

The harp is probably one of the oldest string instruments whose origin goes back to the Prehistory where the first men were charmed by the sound produced by their bow's string. This chordophone was first composed of a few strings attached on an arched frame on one side and on a soundboard on the other side. Then, with the increase of the number of strings, a pillar was added between the neck and the soundboard to support the strings' tension. This kind of harp was particularly used in Europe and marks the origin of the current concert harp. Nowadays, the concert harp is composed of 47 strings, from Cb0 (of fundamental frequency 30.9 Hz) to Gb7 (of fundamental frequency 2960 Hz), attached to the soundboard though an eyelet below which they are knotted. The soundboard is designed to withstand the stress imposed by the strings, as for the Camac concert harp used in this study, which is composed of multiple layers of different materials (aluminium, carbon, woods). From an acoustical point of view, the role of the soundboard is to radiate the sound produced by the vibrations of the strings. To some extent, this sound can also be amplified by the soundbox and its five sound holes [1]. In spite of mechanical and constructional improvements, musicians and harp makers alike are annoyed by the feeling produced by the halo of sound when the instrument is played. When one string is plucked, some others can also be excited by sympathetic vibrations. Although this phenomenon is a fundamental characteristic of the instrument's sound, the instrument maker has to design the harp so that sympathetic vibrations remain reasonable.

The sympathetic couplings between strings lead to the aftersound and sometimes to beats. This arises because some partials of the sound may contain several spectral components whose frequencies are very close one to another. Two kinds of couplings are involved in this situation: couplings between different polarizations of a same string due to the way it is fixed and sympathetic couplings between different strings via the instrument's body [2].

Considering the connection point between a single string and the soundboard as a point, the string/structure interaction can be described by a 6 by 6 admittance matrix. In such a description, three translational degrees of freedom and three rotational degrees of freedom are involved [3]. As a consequence, for one single string, each mode can have up to 6 components, their frequencies being very close one to another in the string's response. However, in practice, 2 components often overshadow the others and correspond to 2 polarizations of the string. This has been shown for the guitar [4], the piano and the violin [5]. The

Received 16 December 2007,
accepted 16 January 2009.

* New address: LAM/IJLRA, CNRS, UPMC Univ. Paris 06, 11 rue de Lourmel, 75015 Paris, France

strong anisotropy of the string/structure interaction (for the out-of-plane and in-plane directions) is responsible for this effect. As a consequence, the decay rates of the two polarizations of a single string are generally different and lead to a double decay effect [2].

Piano strings, which are grouped in pairs or triplet have often served as a model for the study of sympathetic couplings. Such couplings occur because each group of strings (pair or triplet) is practically tuned in unison. The case of two strings tuned in unison having the same polarization, coupled by bridge motion is studied in [2]: normal modes for this configuration appear in pairs and depend on the strings mistuning and bridge admittance. It is the presence of these two coupled modes that is responsible for the phenomena of beats and aftersound. The more complex case of a pair of piano strings tuned in unison, each of them having two polarizations has been studied in [6].

Similar couplings exist in string instruments which do not have pairs of strings tuned in unison. This has been illustrated for the American five-string banjo: in [7], this instrument is modelled by an assembly of one-dimensional sub-systems in which waves propagation occur, allowing the time-domain response to be computed. It is shown that when all the strings are incorporated to the model, the decay time is shorter than when only one string is considered. This is explained by the presence of sympathetically driven strings, even if it is difficult to find out how sympathetic vibrations occur in this model.

For the kantele, which is a Finnish plucked five-string instrument, sympathetic vibrations have also been identified in [8]. Through the experimental analysis of the total amount of energy transferred from one string to all the others, it was shown that the transfer of energy is more pronounced between strings which have simple harmonic relationships.

In a previous paper [9], it was shown that the sympathetic phenomenon is due to the presence of particular modes, called sympathetic modes, in the modal basis of the system. These modes have been both theoretically and experimentally identified on a simple academic configuration close to the harp: two strings tuned to the octave and connected to a beam were considered and the modes of this assembly were investigated. The aim of the present paper is to investigate the sympathetic modes in the response of a real concert harp.

In the first part, a time domain analysis based on a 'High Resolution' method is carried out to identify closely-spaced frequency components present in the fundamental of a single string when plucked. Note that 'High Resolution' techniques are suitable for the spectral analysis of signals having very close spectral components, which cannot be separated using a Fourier analysis because of a lack of resolution. In the second part, the sympathetic vibrations were investigated through the use of a physical model of a simplified concert harp. In the final part, a comparison between theoretical and experimental results give an explanation of the origin of the sympathetic phenomenon in the instrument.

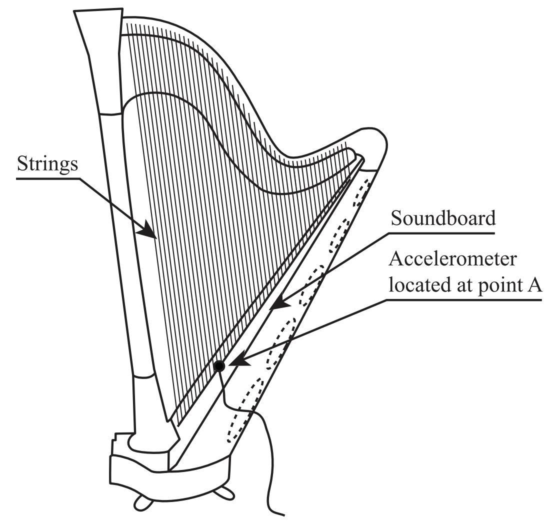

Figure 1. Schematic representation of the experimental setup.

Table I. Characteristics of the experimental configurations. String 24 corresponds to Cb_2 of fundamental frequency 246.92 Hz, string 31 to Cb_3 (123.59 Hz), string 35 to Fb_3 (82.37 Hz), string 38 to Cb_2 (61.52 Hz) and string 42 to Fb_1 (41.08 Hz). All frequencies correspond here to measured frequencies on tuned instrument.

Conf.	Description
(1)	All strings free to vibrate
(2)	All strings damped except string 31
(3)	String 31 stopped during oscillations
(4)	Strings 24, 31, 35, 38 and 42 stopped during oscillations
(5)	Strings 31 and 24 stopped during oscillations
(6)	Strings 31 and 35 stopped during oscillations
(7)	Strings 31 and 38 stopped during oscillations
(8)	String 31 and 42 stopped during oscillations

2. Experimental investigation of the harp's sympathetic modes

2.1. Experimental setup

To highlight the presence of sympathetic modes in the concert harp, the following experimental protocol was used: the harp was plucked in a normal way and an accelerometer mounted on the soundboard at point A was used to measure the induced vibrations (see Figure 1). Point A is located on the inner surface of the soundboard, between the Db_3-string and the Cb_3-string, respectively labelled 30 and 31. The plucked string was string 31 with the other strings either damped or stopped during oscillations. Eight experimental configurations presented in Table I were used to investigate the sympathetic vibrations. The set of strings involved in these configurations is chosen such that the fundamental of string 31 coincides with partials of lower strings.

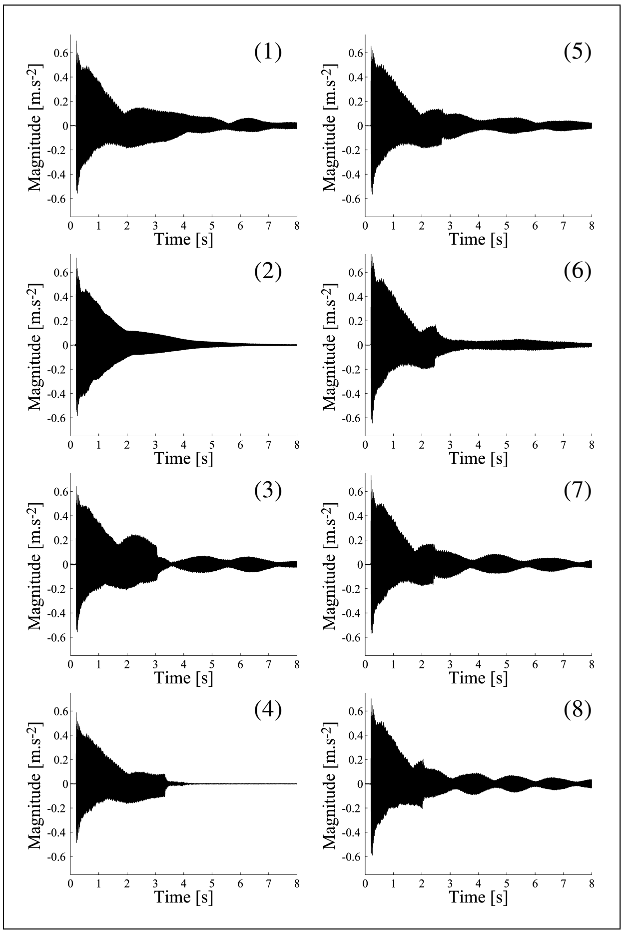

Figure 2. Accelerometer signals measured at point A for the eight experimental configurations defined in Table I.

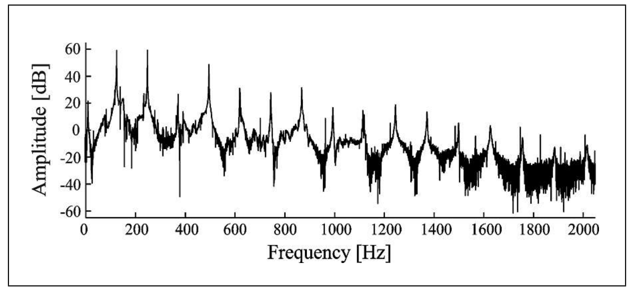

Figure 3. Spectrum of the signal measured at point A when string 31 is plucked.

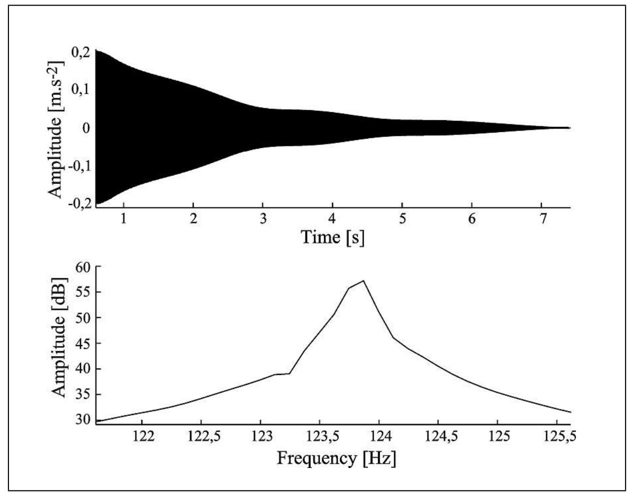

Figure 4. Time waveform and spectrum of the first partial of the vibratory signal measured at point A when string 31 is plucked. All strings are free to vibrate.

The induced vibrations were sampled at 4096 Hz and the decay recorded for 8 seconds. Selected strings were stopped by the harp player a few seconds after plucking string 31. The resulting signals for the eight experimental configurations are shown in Figure 2. These signals highlight a fact well-known by the harpists: stopping of a string plucked does not necessarily imply a fast decrease of the sound level. Indeed, as shown in configurations (3), (5), (6), (7) and (8), the end signal amplitude is of the same order of magnitude that in the free-strings configuration.

2.2. Method used for the extraction of modal parameters

2.2.1. Introduction: limit of the Fourier analysis

String 31 was plucked with all other string free to vibrate and the Fourier spectrum of the accelerometer's signal at point A is shown in Figure 3. Several modes of the coupled system are excited to produce the harp sound. This spectrum is composed of partials which are quasi harmonic. Using an appropriate selective filter, one can zoom-in on the spectrum in the vicinity of the first partial and plot its corresponding time waveform as shown in Figure 4. This figure clearly shows that several sinusoidal components are present in the vibratory signal. The free decay of the response of the instrument after plucking measured by the accelerometer, corresponds to the superposition of several modes whose frequencies are very close one to another. However, the zoomed spectrum does not have the resolution to separate these modes. This illustrates the limitations of Fourier analysis. The presence of closely-spaced modes is a common characteristic in many stringed instruments. Various methods have been applied to musical instruments to resolve this fine structure, such as techniques based on the Hilbert transform [4, 10] or High Resolution methods [4, 11, 12].

For the identification of modes with close frequencies in the first partial, we choose to use a High Resolution method: the ESPRIT algorithm (Estimation of Signal Parameters via Rotational Invariance Techniques) [13]. A brief description of this technique and the specificity of its implementation in our context are given in paragraphs 2.2.2 to 2.2.4. An application to the harp's signals is then presented in section 2.3.

2.2.2. The ESPRIT method

Subspace-based High Resolution methods such as the ESPRIT algorithm are of major interest for estimating mixtures of complex exponentials, because they overcome the spectral resolution limit of the Fourier transform and provide very accurate estimates of the signal parameters. These methods consist in splitting the observations into a set of desired and a set of disturbing components, which can be viewed in terms of signal and noise subspaces. In this framework, the ESPRIT algorithm is based on a particular property of the signal subspace, referred to as the *rotational invariance*. This property permits to extract the model parameters from the eigenvalues of a so-called *spectral matrix*, which is obtained from the estimated signal subspace.

The noiseless Exponential Sinusoidal Model (ESM) defines the discrete signal $x(t)$ as a sum of complex exponentials:

$$x(t) = \sum_{k=1}^{K} a_k e^{\delta_k t} e^{j(2\pi f_k + \varphi_k)}, \quad t \in [0, N-1], \tag{1}$$

where each frequency $f_k \in [-\frac{1}{2}, \frac{1}{2}]$ is associated to a real magnitude ($a_k > 0$), a phase ($\varphi_k \in [-\pi, \pi]$) and a damping or amplification factor ($\delta_k \in \mathbb{R}$). The whole number K is the number of complex exponentials, also called model order, and N is the number of the signal's samples. By defining the complex amplitudes $\alpha_k = a_k e^{j\varphi_k}$ and the complex poles $z_k = e^{\delta_k + j2\pi f_k}$, which are supposed to be distinct, the signal model $x(t)$ can be re-written in the following form:

$$x(t) = \sum_{k=1}^{K} \alpha_k z_k^t. \tag{2}$$

For any time t, the data vector $\mathbf{x}(t) = [x(t), ..., x(t+n-1)]^T$ of dimension $n > K$ belongs to the K-dimensional *signal subspace* spanned by the Vandermonde matrix

$$\mathbf{V}^n = \begin{pmatrix} 1 & 1 & \cdots & 1 \\ z_1 & z_2 & \cdots & z_K \\ \vdots & \vdots & & \vdots \\ z_1^{n-1} & z_2^{n-1} & \cdots & z_K^{n-1} \end{pmatrix}.$$

It can be noted that this Vandermonde matrix satisfies the following rotational invariance property: $\mathbf{V}_\uparrow = \mathbf{V}_\downarrow \mathbf{D}$, where $\mathbf{D} = \mathrm{diag}(z_1 \ldots z_K)$, $\mathbf{V}_\downarrow$ is the matrix extracted from $\mathbf{V}$ by deleting the last row, and $\mathbf{V}_\uparrow$ is the matrix extracted from $\mathbf{V}$ by deleting the first row.

In practice, the measured signal $s(t)$ is corrupted by an additive noise: $s(t) = x(t) + w(t)$, where $w(t)$ is assumed to be white. Although matrix $\mathbf{V}$ is unknown, the signal subspace can still be estimated as the principal eigensubspace of the correlation matrix $\hat{\mathbf{R}}_{ss}$ of the measured signal, defined as follows:

$$\hat{\mathbf{R}}_{ss} = \frac{1}{N-n+1} \mathbf{S}\mathbf{S}^H, \tag{3}$$

where

$$\mathbf{S} = \begin{pmatrix} s(0) & s(1) & \cdots & s(N-n) \\ s(1) & s(2) & \cdots & s(N-n-1) \\ \vdots & \vdots & \ddots & \vdots \\ s(n-1) & s(n) & \cdots & s(N-1) \end{pmatrix} \tag{4}$$

is the $n \times (N-n+1)$ Hankel data matrix which involves N successive samples of the signal and the exponent H is the hermitian conjugate. Thus the $n \times K$ matrix $\mathbf{W}$ formed by the K first principal eigenvectors of $\hat{\mathbf{R}}_{ss}$ is an orthonormal basis of the signal subspace.

Since the matrices $\mathbf{W}$ and $\mathbf{V}$ span the same subspace, there exists a $K \times K$ non-singular matrix $\boldsymbol{G}$ such that $\mathbf{V} = \mathbf{W}\mathbf{G}$. It can then be noted that $\mathbf{W}$ satisfies an invariance property similar to that of the Vandermonde matrix: $\mathbf{W}_\uparrow = \mathbf{W}_\downarrow \mathbf{\Phi}$, where the $K \times K$ matrix $\mathbf{\Phi} = \boldsymbol{G}\boldsymbol{D}\boldsymbol{G}^{-1}$, referred to as the *spectral matrix*, is similar to the diagonal matrix $\mathbf{D}$. In particular, the eigenvalues of $\mathbf{\Phi}$ are the complex poles z_k.

Finally, the ESPRIT algorithm consists of the following steps:

1. compute the signal subspace basis $\mathbf{W}$ by means of an eigenvalue decomposition,
2. compute the spectral matrix $\mathbf{\Phi}$ by means of the least squares method:

   $$\mathbf{\Phi} = \mathbf{W}_\downarrow^+ \mathbf{W}_\uparrow, \tag{5}$$

   where the symbol $^+$ denotes the Moore-Penrose pseudo-inverse,
3. estimate the complex poles z_k as the eigenvalues $\mathbf{\Phi}$.

It is proved that the best performance in terms of statistical efficiency is obtained for a proper dimensioning of the data matrix $\mathbf{S}$: $n = N/3$ or $n = 2N/3$ [12].

In a second stage, the complex amplitudes α_k, grouped in a $K \times 1$ vector denoted α, are obtained thanks to the least squares method:

$$\alpha = [\mathbf{V}^N]^+ s. \tag{6}$$

In equation (6), s denotes the vector containing N successive samples of the signal and $\mathbf{V}^N$ is the $N \times K$ Vandermonde matrix defined by the poles estimated by the ESPRIT method. Parameters a_k and φ_k are directly deduced as the modulus and phase of the complex amplitudes α_k.

2.2.3. Estimation of the number of components

The main difficulty of the method consists in evaluating the number K of components present in the signal. The technique commonly used is the over-estimation of this number and the discrimination of spurious results by means of an indicator such as the components energy or the error between the measured signal and the model. Other more effective methods exist for estimating the model order K such as the ESTimation ERror (ESTER) method [12, 14] also used in the study. It consists in the computation of an inverse error function,

$$\boldsymbol{J} : p \mapsto \frac{1}{\| \mathbf{E}(p) \|_2^2}, \tag{7}$$

where

$$\mathbf{E}(p) = \mathbf{W}_\uparrow(p) - \mathbf{W}_\downarrow(p)\mathbf{\Phi}(p) \tag{8}$$

for all possible orders $0 < p < n-1$. For determining the value of K, we choose the greatest value of p for which the function $\boldsymbol{J}(p)$ reaches a maximum which is greater than a threshold chosen arbitrarily above the noise level contained in the signal.

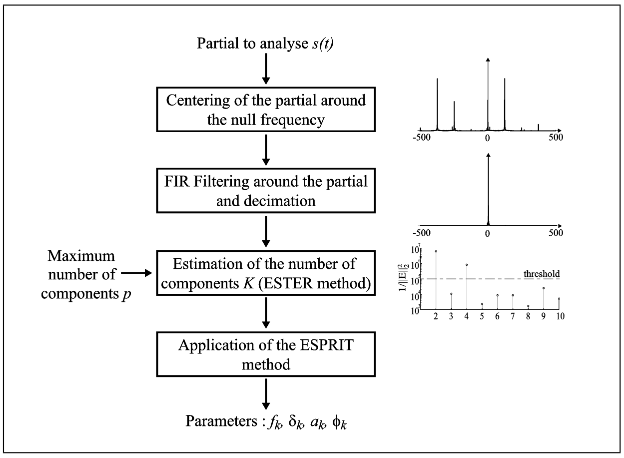

Figure 5. Summary of the implementation of the ESPRIT method on the studied partial.

2.2.4. ESPRIT method implementation

In order to minimize the computational time and increase the results accuracy [12], the ESPRIT method implementation is carried out according to the following procedure: after centering the studied partial around the null frequency, a finite impulse response (FIR) filter selects the frequency range containing the partial to analyse. The filter is chosen with a linear phase to keep the signal waveform. The filter is known to have a finite transitory response which corresponds to the length of its impulse response. The first filtered signal points belonging to this transitory phase are thus removed from the processing afterwards [4]. The filtered and centered signal is highly decimated to limit the computational time of the ESPRIT method. After the estimation of the model order by the ESTER method, as previously explained in section 2.2.3, the ESPRIT algorithm is then applied. The final validation of the model order is performed using a comparison between the measured and synthesized signals. An illustration of the method implementation is shown in Figure 5.

Note that in the Exponential Sinusoidal Model, the signal is assumed to be complex. For a musical sound, the signal is real and can be written as follows:

$$x(t) = \sum_{k=1}^{K} A_k e^{\delta_k t} \cos(2\pi f_k t + \varphi_k), \tag{9}$$

which can be re-written with exponential terms:

$$x(t) = \sum_{k=1}^{K} \frac{A_k}{2} e^{\delta_k t} e^{j(2\pi f_k t + \varphi_k)} + \sum_{k=1}^{K} \frac{A_k}{2} e^{\delta_k t} e^{-j(2\pi f_k t + \varphi_k)}. \tag{10}$$

Because of the filtering in the spectrum around the studied partial, the studied signal corresponds to the first part (with positive frequency) of the equation (10). In order to find the real amplitude of the measured signal, the amplitude A_k obtained by the ESPRIT method has to be multiplied by two.

2.3. Results

The implemented ESPRIT method, as previously explained, is applied to the signals measured on the concert harp in its final part, between 4s and 8s. The different experimental conditions are described in Table I and the attention is focused on the first partial of string 31. The estimated components found for this partial are gathered in Table II. The model order stretches from 0, for configuration (4), to 4, for configuration (1). The observed modal frequencies and damping were computed from 5 measurements to estimate uncertainty. In Table II, the components are classified in such a way that their amplitude are in descending order from top to bottom. Moreover, they are aligned to facilitate the cognition of missing components.

The repeatability uncertainties for different parameters are extremely small, lower than 1% for the frequencies and around 10% for the damping factors. Nevertheless, for some components the uncertainty can be important as for the last component of the (1) configuration. This can happen for weakly excited modes with a weak signal-to-noise ratio.

When the instrument is not modified ((1) and (3) to (8) configurations) the components' parameters slightly vary, less than 0,5% for the frequencies and, a maximum of 30% of variation in the damping factors. This shows that the stopped string does not modify the vibratory behavior of the instrument. Nevertheless, when paper is added to damp all strings except string 31, in configuration (2), the frequency and damping of the plucked string are modified and a slight shift in frequency is caused, but not enough to allow the identification of the components' nature. Thanks to the developed experimental protocol and the identification method, the components present in the first partial are obtained. The estimated modal parameters are stable in all eight experiences. These results are compared in the following section to the predicted modes of one simplified harp model.

3. Theoretical study of the harp's sympathetic modes

3.1. Description of the model

The vibrations of the concert harp used in our measurements were investigated in a previous paper [1] using an experimental modal analysis. At low frequencies, six consecutive modes were identified from 24 Hz to 181 Hz. For all modes, mode shapes were symmetric relative to the string plane and with the bending of the soundboard similar to the first mode shape of a beam clamped at both ends. Thus, although the soundboard is a complex assembly, consisting of a sandwich of several layers of different wood glued together reinforced by a central aluminum bar and two lateral stiffeners in wood, the soundboard can be described by using an equivalent beam clamped at both ends. The typical first bending mode at 152.2 Hz is shown in Figure 6-A. Its corresponding mode shape can schematically be described as an important deflection in the lower

Table II. Frequencies and damping factors of identified components in the first partial of the accelerometer signals in the eight experimental configurations defined in Table I. The reported uncertainty is an uncertainty with a 95% confidence interval.

	Configurations							
	(1)	(2)	(3)	(4)	(5)	(6)	(7)	(8)
Components	123.59±0.01 -0.68±0.02	123.54±0.01 -0.57±0.01						
	123.34±0.01 -0.15±0.03		123.35±0.00 -0.11±0.01		123.34±0.00 -0.11±0.01	123.34±0.00 -0.11±0.01	123.30±0.01 -0.10±0.01	
	123.08±0.00 -0.26±0.01		123.09±0.01 -0.21±0.01		123.08±0.00 -0.22±0.03	123.08±0.00 -0.21±0.02		123.09±0.01 -0.22±0.07
	123.78±0.02 -0.15±0.12	123.71±0.03 -0.54±0.06						

two thirds of the soundboard between the two clamped points, one at the pillar level and the other one at the 11-string level. For the treble strings, the rigidity of the soundboard is increased by the proximity of the edges of the soundbox, explaining the absence of movement at low frequencies. Thus, the beam length is limited to the distance between the harp's pillar and the 11th string. We therefore model the soundboard as a 1m-long beam on which 35 strings are attached as shown in Figure 6-B.

The mechanical properties of the equivalent beam and of each string have to be determined: for the strings, most parameters are directly measured on the harp [15] except for the Young's modulus and the density which are supposed to equal the data given in [16] and [17]. Values of the tension are computed from the fundamental frequency of the tones, by considering the strings as rigidly fixed at both ends, in such a way that the string's mode frequency corresponds to the one directly measured on the harp. For the equivalent beam, the determination of its parameters is more complicated since the geometrical parameters are directly measured on an isolated soundboard, allowing the evaluation of a mean density ($\rho = 553\,\mathrm{kg/m^3}$). The area of the cross-section A and the second moment of area J were measured at different positions along the axis. Averages values of these two parameters are thus retained to characterize the equivalent beam ($A_{eq} = 38.3$ cm^2 and $J_{eq} = 38.9\,\mathrm{cm^4}$). Finally, the Young's modulus E ($E = 5.9\,\mathrm{GPa}$) of the equivalent beam was adjusted to give the first observed bending mode of the beam at 150 Hz in the beam-35 strings assembly. This was the fourth mode shown in Figure 6A. We refer to this simplified model as the simplified harp.

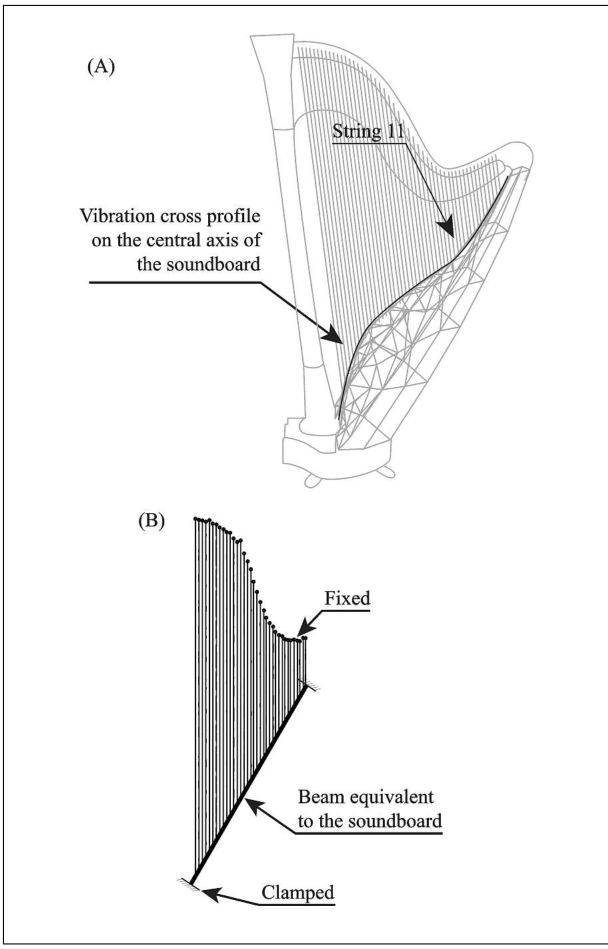

Figure 6. (A) Modal shape associated to the fourth mode and description of the vibratory profile in the central axis of the soundboard. (B) Model of the concert harp: beam-35 strings assembly.

3.2. Harp's sympathetic modes

The normal modes of vibration of the simplified harp were computed using the transfer matrix method, appropriate for modeling assemblies of one-dimensional substructures. The computation was based on a wave-guide model for each sub-structure of the beam-strings assembly. The different steps of the method are developed in details in [9]. Eigenfrequencies were obtained by identifying the singularities of a characteristic matrix labeled R_R (see equation (30) in [9]). Each drop of the logarithm of matrix R_R's determinant corresponds to an eigenfrequency.

The normal modes of the simplified harp were computed in the frequency range [0-500 Hz] in steps of 0.01 Hz. The logarithm of matrix R_R's determinant is shown in Figure 7 in the frequency range [110-160 Hz], exhibiting well defined, closely spaced eigenfrequencies. Among the 151 modes found in the range [0-500 Hz], ex-

Table III. Eigenfrequencies and Kinetic Energy Ratio for each sub-structure (strings 42, 38, 35, 31, 24 and the beam). KER expressed in % and rounded to the nearest whole number.

Mode	Frequency (Hz)	KER (%) string 42	string 38	string 35	string 31	string 24	Beam
26	122.95	0	99	0	1	0	0
27	123.29	97	1	0	2	0	0
28	123.59	0	0	0	100	0	0
33	149.91	0	0	1	0	0	73

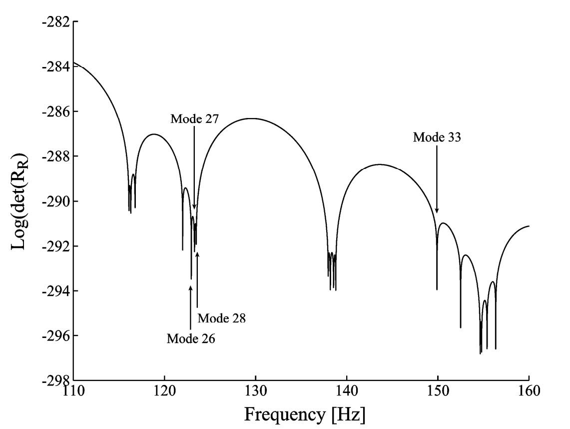

Figure 7. Logarithm of the determinant of the characteristic matrix R_R as function of frequency. Each drop corresponds to an eigenfrequency of the beam-strings assembly.

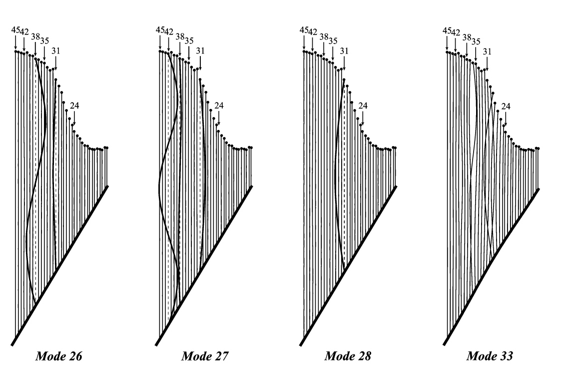

Figure 8. Mode shapes associated to modes 26, 27, 28 and 33. The number indicated below the harp's arm points out the string number.

amples of four modal shapes are presented in Figure 8. These shapes illustrate normal modes of the harp involving the coupled vibrations of strings which share partials having closely similar frequencies. To classify modes of the assembly, we define a criterion called Kinetic Energy Ratio (KER)

$$KER_j(k) = \frac{\displaystyle\int_0^{l_k} \rho_k \mathbf{\Psi}_j^T(x)\mathbf{\Psi}_j(x)\,\mathrm{d}x}{\displaystyle\sum_r \int_0^{l_r} \rho_r \mathbf{\Psi}_j^T(x)\mathbf{\Psi}_j(x)\,\mathrm{d}x}. \qquad (11)$$

In this equation ρ is the mass per unit length of the sub-structure, $\mathbf{\Psi}_j$ is the mode shape of mode j and x is the generic space variable. The KER corresponds to the ratio of kinetic energy of one sub-structure k (of length l_k) divided by the total kinetic energy of the structure. Its value is a percentage and allows us to identify the relative importance of each sub-structure displacement field. In the study, this percentage is rounded to the nearest whole number. Thus, for a given mode, a null value of the KER of a sub-structure indicates that this sub-structure is inactive. Values of KER on each sub-structure are used to classify the modes into four groups [9]: beam modes, string modes, string-string modes, and beam-string modes.

In Table III, the predicted eigenfrequencies and KER for modes 26, 27, 28 and 33 are reported. For the three first modes, the KER is significant only for four sub-structures: the beam and strings 31, 38 and 42. String 31 (Cb_3 note of fundamental frequency 123.59 Hz) corresponds to the upper octave of string 38 (Cb_2 note at fundamental frequency 61.52 Hz). String 42 (Fb_1 at fundamental frequency 41.08 Hz) is an octave and a fifth below string 31. The uncoupled frequencies of the strings are harmonically related in the ratio 1, 2 and 3. For modes 26 to 28, the KER for the beam is extremely small, showing that mode shapes are dominated by the string's motion, allowing the definition of these modes as string-string modes or sympathetic modes [9]. According to the modal superposition principle, if string 31 is plucked, all normal modes participate to the response. Vibrations of strings 38 and 42, which are involved in the modes 26 and 27 are thus induced. Such motions correspond to sympathetic vibrations. Note that for the modes 26 to 28, modifications of the characteristics of the equivalent beam only slightly modify the KER distribution, not altering our conclusions.

4. Discussion

When string 31 of the concert harp is free to oscillate (configuration (1) in Table I), 4 sinusoidal components are identified in the first partial. When string 31 vibrate with all other strings damped (configuration 2), only two of these 4 components remained. These two components have close frequencies, separated by only 0.19 Hz, but have very different damping factors and amplitudes. This arises because the two polarizations of transverse string vibration are excited by the harp player depending on how the string is plucked, involving different initial amplitudes

Table IV. Comparison between experimental and theoretical results obtained from the vibratory model of the concert harp for String 31 mode and Sympathetic modes 31-42 and 31-48.

	Modal frequency		
	Experimental	Theoretical	Error
String 31	123.59 Hz 123.78 Hz	123.59 Hz	
31-42	123.34 Hz	123.29 Hz	0.04 %
31-38	123.08 Hz	122.95 Hz	0.11 %

(showed by the difference of energy of each component). As for the piano, one of the polarizations (with its plane of polarisation perpendicular to the soundboard) can transmit energy to the soundboard, implying a rapidly decaying component at the plucking moment while the string vibration parallel to the flat surface of the soundboard is weakly coupled to the soundboard [2]. Complete modelling of the strings' modal behavior requires that both polarizations of string vibrations have to be taken into account. In our simplified harp model, only one polarization is considered.

When a particular string is stopped during the oscillations, any modes involving large amplitude vibrations of that string will be quickly damped. In configurations (3), string 31 stopped during oscillations, (5), strings 31 and 24 stopped during oscillations, and (6), strings 31 and 35 stopped during oscillations, the same components are present, showing that modes involving the vibrations of strings 24 and 35 do not participate in the first partial of the instrument response. By stopping strings 31 and 38, one vibrating component disappears and by stopping strings 31 and 42, another one is absent from the instrument's response. With configurations (7) and (8), we can deduce that strings 38 and 42 participate in the sound radiated by the instrument.

When the harpist plucks string 31, four modes are set into vibrations at the same time: two modes involving string 31 (one mode per polarization at 123.59 Hz and 123.78 Hz), one mode involving the fundamental of string 31, coupled to the second partial of string 38 (123.08 Hz) and one mode involving strings 31 coupled to the third partial of string 42 (123.34 Hz). These last two modes are thus the sympathetic modes. The stopping of string 31 does not necessary lead to the weakening of these modes, proving that for these modes the kinetic energy in strings 42 and 38 is more important than in string 31. Moreover, these results show that sympathetic modes associated with the weakly coupled transverse vibrations of string 31 are not visible in the response. Such modes will only be weakly excited, not allowing them to emerge from the noise

Our experimental results can be compared to those obtained from the theory. In our simplified harp model, the value of the string's tension is evaluated in such a way that the string's mode's frequency corresponds to the measured value of the partial (123.59 Hz in the studied example). To do so, the beam-strings model is computed as many times as necessary to meet the correct frequencies. The comparison between the eigenfrequencies of the theoretical and experimental coupled modes is presented in table IV. Since the target value for the fitting procedure is 123.59 Hz, this value is the same for theoretical and experimental results. For sympathetic modes 31-42 and 31-38, their eigenfrequencies are measured at 123.34 Hz and at 123.08 Hz. It should be noticed that the theoretical eigenfrequencies of these modes are found at 123.29 Hz and at 122.95 Hz, coinciding almost perfectly with experimental results. Apart from the fact that the vibratory model of the concert harp does not take the two polarizations of the string into account, results obtained from the model are in very good agreement with those obtained from experiments, thus validating the use of our simplified model of the beam-35 strings assembly of the concert harp.

5. Conclusion

The numerous strings of the concert harp induce sympathetic vibrations, which are responsible for the halo of sound in the decay of the plucked note. This characteristic is important and constitutes a signature of the sound of the instrument. In this paper, experimental and theoretical investigations have been carried out to understand this phenomenon. The following conclusions can be drawn.

a) Normal modes of the string-soundboard assembly include contributions from the upper partials of simply related lower strings. Such modes explain the existence of sympathetic string vibrations. Using a wave-guide model of a simplified harp, the eigenfrequencies and mode shapes of such modes can be accurately determined. This model describes bending and longitudinal motions in the strings, connected to an equivalent beam representing the soundboard and allows the modal basis of the strings-beam assembly to be computed.

(b) In the time domain, sympathetic vibrations generate multiple components in the string's partials. Resolution of the Fourier analysis does not permit their identification. This identification is performed using the ESPRIT method, which is a High Resolution method. The determination of the number of elementary spectral components, which is the main difficulty in the implementation of High Resolution methods is successfully performed using the ESTER method.

(c) Several components contribute in the first partial of string 31: two of them correspond to the string having two different polarizations. Other components correspond to sympathetic modes. In the analysed example, two sympathetic modes are involved. Their number and their eigenfrequencies are very well captured by the proposed model.

Although the model of the instrument suits the identification of sympathetic modes, it can be extended in order to take into account two polarizations per strings. Moreover, from an experimental point of view, the analysis of partials of higher order, where other phenomena such as octave vibrations can be present, could also be performed.

Acknowledgement

The authors acknowledge the instrument maker Camac Harps for the lending of the concert harp. The research leading to this paper was partly supported by the French GIP ANR under contract ANR-06-JCJC-0027-01, Décomposition en Éléments Sonores et Applications Musicales - DESAM.

References

[1] J.-L. Le Carrou, F. Gautier, E. Foltête: Experimental study of A0 and T1 modes of the concert harp. J. Acoust. Soc. Am. **121** (2007) 559–567.

[2] G. Weinreich: Coupled piano strings. J. Acoust. Soc. Am. **162** (1977) 1474–1484.

[3] X. Boutillon: Measurement of the three-dimensional admittance at a violin bridge. Proceedings of the 13th International Congress of Acoustics, Belgrade, Serbia, 1989.

[4] B. David: Caractérisations acoustiques de structures vibrantes par mise en atmosphère raréfiée. Méthodes d'estimation relatives aux fréquences et amortissements des modes propres. Applications en acoustique musicale (Acoustical characterization of vibrating structures in near vacuum. Estimation methods for eigenfrequencies and damping factors. Applications in Musical Acoustics). PhD Thesis, Université Paris 6, Paris, France, 1999.

[5] N. H. Fletcher, T. D. Rossing: The physics of musical instruments. Springer Verlag, New York, 1991.

[6] B. Capleton: False beats in coupled piano string unisons. J. Acoust. Soc. Am. **115** (2004) 885–892.

[7] J. Dickey: The structural dynamics of the American five-string banjo. J. Acoust. Soc. Am. **114** (2003) 2958–2966.

[8] C. Erkut, M. Karjalainen, P. Huang, V. Välimäki: Acoustical analysis and model-based sound synthesis of the kantele. J. Acoust. Soc. Am. **112** (2002) 1681–1691.

[9] J.-L. Le Carrou, F. Gautier, N. Dauchez, J. Gilbert: Modelling of sympathetic string vibrations. Acta Acustica united with Acustica **91** (2005) 277–288.

[10] L. Rossi, G. Girolami: Instantaneous frequency and short term Fourier transforms: Application to piano sounds. J. Acoust. Soc. Am. **110** (2001) 2412–2420.

[11] J. Laroche: The use of the matrix pencil method for the spectrum analysis of musical signals. J. Acoust. Soc. Am. **94** (1993) 1958–1965.

[12] R. Badeau: Méthodes à haute résolution pour l'estimation et le suivi de sinusoides modulées. Application aux signaux de musique. (High resolution methods for estimating and tracking modulated sinusoids. Application to music signals). PhD Thesis, Télécom Paris, Paris, France, 2005.

[13] R. Roy, A. Paulraj, T. Lailath: ESPRIT - A subspace rotation approach to estimation of parameters of cisoids in noise. IEEE Transactions on Acoustics, Speech and Signal Processing **34** (1986) 1340–1344.

[14] R. Badeau, B. David, G. Richard: A new perturbation analysis for signal enumeration in rotational invariance techniques. IEEE Transactions on Signal Processing **54** (2006) 450–458.

[15] J.-L. Le Carrou: Vibro-acoustique de la harpe de concert (Vibro-acoustics of the concert harp). PhD Thesis. Université du Maine, Le Mans, France, 2006.

[16] A. J. Bell, I. M. Firth: The physical properties of gut musical instrument strings. Acustica **60** (1986) 87–89.

[17] A. J. Bell: An acoustical investigation of the Concert Harp. PhD dissertation, University of St Andrews, United Kingdom, 1987.